Isomorphous Crystal Structures of *Escherichia coli* Dihydrofolate Reductase Complexed with Folate, 5-Deazafolate, and 5,10-Dideazatetrahydrofolate: Mechanistic Implications[†,‡]

Vicente M. Reyes, Michael R. Sawaya, Katherine A. Brown,[§] and Joseph Kraut*

Department of Chemistry and Biochemistry, University of California, San Diego, La Jolla, California 92093-0317

Received September 27, 1994; Revised Manuscript Received December 8, 1994[⊗]

ABSTRACT: Crystal structures of *Escherichia coli* dihydrofolate reductase (ecDHFR, EC 1.5.1.3) in binary complexes with folate, 5-deazafolate (5dfol), and 5,10-dideazatetrahydrofolate (ddTHF) have been refined to *R*-factors of 13.7%, 14.9%, and 14.5%, respectively, all at 1.9 Å. All three are isomorphous with a previously reported binary complex of ecDHFR with methotrexate (MTX), in space group $P6_1$, two molecules per asymmetric unit [Bolin, J. T., Filman, D. J., Matthews, D. A., Hamlin, R. C., & Kraut, J. (1982) *J. Biol. Chem. 257,* 13650−13662]. A hitherto unobserved water molecule is hydrogen bonded to the pteridine N5 and O4 in both molecules of the asymmetric unit of the folate complex (but not the 5dfol or ddTHF complexes), supporting the hypothesis that N5 protonation of bound substrate, an important step of the DHFR reaction, occurs by way of such a water molecule. There is no indication of a hydrogen bond between N8 of 5dfol and the backbone carbonyl of Ile-5, suggesting that the bacterial enzyme, unlike the human enzyme [Davies, J. F., II, Delcamp, T. J., Prendergast, N. J., Ashford, V. A., Freisheim, J. H., & Kraut, J. (1990) *Biochemistry 29,* 9467−9479], does not favor protonation at N8. Perhaps this explains why bacterial DHFR is much less effective than vertebrate DHFR in folate reduction. When the ecDHFR·NADPH complex (space group $P3_221$; M. R. Sawaya, in preparation) is superimposed on the folate and 5dfol complexes, the distances from pteridine C6 to nicotinamide C4 were found to be 2.9 and 2.8 Å, respectively, in close agreement with the theoretically calculated optimal distance in the transition state for hydride transfer [Wu, Y. D., & Houk, K. N. (1987) *J. Am. Chem. Soc. 109,* 906−908, 2226−2227]. In contrast to the planar ring system of folate or 5dfol, the reduced pteridine ring of ddTHF is severely puckered and bent toward the nicotinamide pocket, with the reduced pyridine ring assuming a half-chair type of conformation. This change in shape causes the pteridine ring to bind with O4 closer to Trp-22(Nε1) by over 0.5 Å, so that an invariant water molecule now bridges these two atoms with ideal hydrogen bonds. Furthermore, while the pABA rings of folate and 5dfol are nearly coincident and closer to the αC helix than to the αB helix, those of MTX and ddTHF are displaced along the binding crevice by approximately 1.1 and 0.6 Å, respectively, and are equidistant from αB and αC. These two features could explain the slow release of THF from the enzyme−product complex. Finally, when the NADPH complex is superimposed with the ddTHF complex, we find a full 2.0 Å van der Waals overlap between the pteridine C7 and nicotinamide C4, perhaps explaining the acceleration of THF release by cofactor binding.

Dihydrofolate reductase (DHFR)[1] is a ubiquitous enzyme necessary for normal cellular metabolism in both prokaryotic and eukaryotic cells [for reviews, see Blakley (1984), Freisheim and Matthews (1984), Kraut and Matthews (1987), and Blakley and Appleman (1994)). DHFR catalyzes the NADPH-dependent reduction of 7,8-dihydrofolate (DHF) to 5,6,7,8-tetrahydrofolate (THF) and, much less efficiently, of folate to THF. The latter, in turn, is a key coenzyme that serves as a carrier for the mobilization and transfer of one-carbon fragments in a variety of cellular biosynthetic pathways. For example, the conversion of glycine to serine and synthesis of methionine from homocysteine require the participation of $N^{5,10}$-methylene-THF and N^5-methyl-THF, respectively. In rapidly proliferating cells, such as cancer cells, DNA synthesis is significantly elevated, and hence there is an increased demand for dNTPs, one of which is dTTP. The usual biosynthetic route to thymidylic acid, its precursor, is via methylation of deoxyuridylic acid, a process which cannot take place without the participation of $N^{5,10}$-methylene-THF. This reaction depends on THF not only as a one-carbon fragment carrier but also as a source of reducing equivalents, for THF is oxidized to DHF in the process. Thus rapidly proliferating cells are especially sensitive to the cellular level of DHFR, which is required to maintain a viable cellular level of THF. Methotrexate

[†] Supported by NIH Grant CA 17374.

[‡] Coordinates for the 5dfol, folate, ddTHF, and NADPH complexes have been deposited in the Brookhaven Protein Data Bank under the file names 1DYH, 1DYI, 1DYJ, and 1DRH, respectively.

* Author to whom correspondence should be addressed.

[§] Present address: Department of Biochemistry, Imperial College, London SW7 2AY, U.K.

[⊗] Abstract published in *Advance ACS Abstracts,* February 1, 1995.

[1] Abbreviations: 5dfol, 5-deazafolate; clDHFR, chicken liver DHFR; ddTHF, 5,10-dideazatetrahydrofolate; DHF, 7,8-dihydrofolate; DHFR, dihydrofolate reductase; ecDHFR, *Escherichia coli* DHFR; F_c, calculated structure factor; F_o, observed structure factor; huDHFR, human DHFR; Ile-5(O), backbone carbonyl oxygen of Ile-5; Ile-7(O), backbone carbonyl oxygen of Ile-7; Ile-94(O), backbone carbonyl oxygen of Ile-94; MTX, methotrexate; pABA, *p*-aminobenzoic acid; pABG, *p*-aminobenzoyl glutamate; THF, 5,6,7,8-tetrahydrofolate; Trp-22(Nε1), the Nε1 atom of the Trp-22 side chain.

0006-2960/95/0434-2710$09.00/0

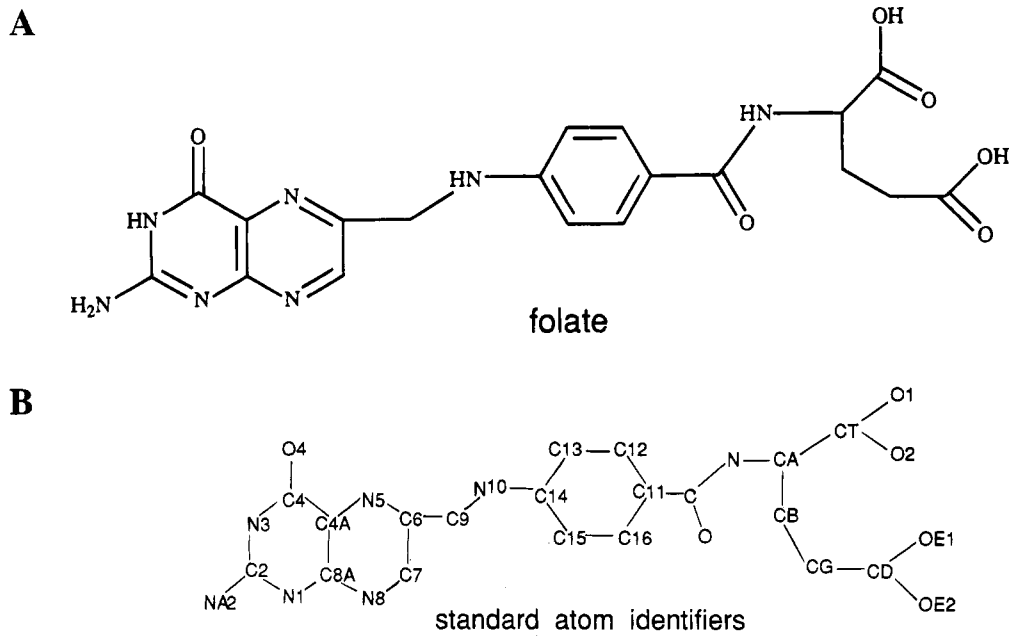

FIGURE 1: (A) Structural formula of folate. (B) Standard atom identifiers. The molecule is composed of three sections: the pteridine ring (all atoms to the left of C9), the pABA moiety (from N10 to C=O), and the glutamate residue (N and all atoms to the right of it). In DHF, C7−N8 is a single bond (with a hydrogen at N8), while in THF both C7−N8 and N5−C6 are single bonds (with hydrogens at both N5 and N8). In 5dfol, N5 is replaced by C5, and in ddTHF both N5 and N10 are replaced by C5 and C10. In MTX, N3−C4 is a double bond, O4 is replaced by the amino group NA4, and N10 is methylated.

(MTX), a potent inhibitor of DHFR [for a review on DHFR inhibitors, see Kuyper (1989)], is consequently an effective anticancer and antitumor agent.

The structural formula of folate is depicted in Figure 1. The molecule is tripartite, composed of a substituted pteridine ring (pterin), a central *p*-aminobenzoic acid (pABA) segment, and a glutamate residue. The pABA and the glutamate together make up the *p*-aminobenzoyl glutamate (pABG) moiety (sometimes referred to as the "tail"). The pterin ring is itself made up of a 4-oxo-2-aminopyrimidine ring fused with a pyrazine ring, the latter being the moiety where reduction takes place. In the derivative 5dfol, N5 of folate has been replaced by C5, whereas in the derivative ddTHF, N5 and N10 of THF have been replaced by C5 and C10.

The ecDHFR enzyme is composed of 159 amino acid residues, and its overall three-dimensional structure is dominated by a central eight-stranded mixed β sheet with a single penultimate antiparallel strand; it contains as well four α helices and five loops. The substrate binding site is primarily hydrophobic but is marked by the presence of a single ionizable residue, Asp-27, which is highly conserved and important for catalytic activity at neutral pH (Howell et al., 1986). The cofactor binding site is proximal to the substrate binding site, and its dihydronicotinamide pocket is lined with coplanar oxygen groups which presumably function to stabilize the transition state of the nicotinamide ring. At the entrance to the pterin and nicotinamide binding sites is a flexible loop (the "Met-20 loop") which acts as a lid apparently controlling the entry and exit of ligands. Conformational changes in this loop are thought to trigger further conformational changes elsewhere which ultimately transform the ground-state Michaelis−Menten complex into the transition-state complex (Li et al., 1992).

An immediate mechanistic goal of the enzyme is to develop a partial positive charge at C6 of the substrate to promote hydride transfer from C4 of the cofactor's dihydronicotinamide ring. This may be assisted by protonation of N5, and an obvious candidate for involvement in this process is Asp-27. However, Asp-27 is 5 Å from N5 and is hydrogen bonded, not to N5, but to NA2 and N3, so its role is something of a mystery. There are currently two models for the mechanism of proton donation to N5. The earlier version (Bystroff et al., 1990; Brown & Kraut, 1992) postulates that Asp-27 is involved in a proton relay from pteridine N3 to O4, via a fixed water molecule, which results in the enolization of O4. The enolized O4, stabilized via the Gandour effect (Gandour, 1981), is supposed then to relay its proton via a water molecule that slips under the Met-20 loop and which is the ultimate proton donor to N5. Using NMR techniques, however, it was recently demonstrated that pteridine O4 is *not* enolized in the ground state (Blakley et al., 1993). (Nevertheless, note that these experiments cannot rule out the possibility of enolization at O4 in the transition state.) Still more recently, moreover, difference Raman spectroscopy has shown that when the cofactor is also bound, the pK_a of the bound pteridine N5 is 6.5 (Chen et al., 1994), as compared with 2.6 in solution (Maharaj et al., 1990). Perhaps the role of Asp-27 is to remain ionized and simply to raise the pK_a of N5 via a long-range electrostatic effect. In any case these new data suggest that N5 may be able to accept a proton directly from the bulk solvent via a network of water molecules that extend from the active site cavity to the protein exterior (McTigue et al., 1992, and observations described later). Whichever model is correct, a water molecule must closely associate with pteridine N5 at some stage in the reaction to serve as the final proton donor to N5. Upon reclosing of the floppy Met-20 loop, this transient water molecule would be forced out, leaving a positive charge at N5, which then may delocalize to the neighboring C6 where it would be stabilized by the partial negative charge on Ile-94(O) located close by. Then, with the nicotinamide C4 and the pteridine C6 held in sub-van der Waals contacts as they bind to the enzyme, hydride transfer will be facilitated.

Our goal is to gather evidence in support of and possibly to extend the model for transition-state formation proposed

by Bystroff et al. (1990). One approach would be to determine the structure of DHFR complexed with folate and analogs in relevant states of reduction, as well as with ligands corresponding to fragments of the substrate. In the present study we report the structures of ecDHFR complexed with folate, 5dfol, and ddTHF, all in the same crystal form. It should be emphasized that this latter consideration is important since we wish to minimize possibly misleading structural effects due to crystal packing differences.

The choice of substrate and product analogs in this study is based on the following information. It is well established that vertebrate DHFR can catalyze the reduction of folate more efficiently than does bacterial DHFR. Since reduction of folate probably requires protonation of pteridine N8 and subsequent or concerted hydride transfer to C7, it would be reasonable to expect that vertebrate DHFR can more effectively protonate pteridine N8. The crystal structure of huDHFR complexed with 5dfol (Davies et al., 1990) supports this hypothesis: 5dfol is indeed protonated at N8 in this complex, even though folate itself is not. The reason is simply that the pK_a of N8 is expected to be substantially higher in 5dfol than in folate, just as the pK_a of pyridine, 5.2, is substantially higher than the pK_a of pyrazine, 0.6 (Weast, 1968). One is thus prompted to ask whether bacterial DHFR is so much less efficient at reducing folate simply because it cannot as readily protonate N8. The crystal structure of ecDHFR complexed with 5dfol can potentially answer this question: if N8 is indeed protonated, it should, by analogy with the huDHFR•5dfol structure, hydrogen bond to Ile-5(O), which ought to be clear from the crystal structure. As for ddTHF, it is structurally similar to the product of the DHFR reaction, THF, the only difference being the C for N substitutions at positions 5 and 10. The structure of the complex with ddTHF should thus yield information about the enzyme−product complex, which may be useful in explaining the slow product-off kinetics of DHFR. Additionally, one expects the transition-state structure of the substrate to lie somewhere between that of DHF and THF and thus to be closer to THF than to folate. This is another reason the structure of the enzyme−product complex could be helpful.

MATERIALS AND METHODS

DHFR Preparation and Purification. Cloned ecDHFR protein was expressed in *Escherichia coli* strain CV634 harboring the p9-3-derived plasmid, pCV29, which encodes the wild-type ecDHFR gene; cell growth, protein extraction, concentration, and purification were as previously described (Smith & Calvo, 1980, 1982). The purified protein was stored at 4 °C in high-salt buffer containing 10 mM Tris-HCl, pH 7.3, 1 mM K_2EDTA, pH 7.3, 0.2−0.5 M KCl, and 0.2 mM DTE. A few days before crystallization, approximately 10 mg of DHFR was dialyzed against 1.0 L of 0.1 M Tris, pH 7.0, at least four times for 3−4 h. After dialysis the absorbance of the protein at 260 and 280 nm was read to determine its concentration. The ligand was then added in powdered form at 3 molar excess; the solution was swirled gently and stored overnight at 4 °C wrapped in aluminum foil to minimize photodegradation. The protein complex was concentrated in a Centricon-10 protein concentrator (Amicon Corp., Beverly, MA) which had been thoroughly washed with 0.1 M Tris, pH 7.0, until the protein concentration was approximately 40−60 mg/mL. Protein concentrations were estimated from solution volumes. This concentrated solution was then stored in the dark at 4 °C until ready for crystallization.

Table 1: *E. coli* DHFR Bindary Complex Crystals: Crystallographic Data Collection and Refinement Statistics[a]

	folate	5dfol	ddTHF
a, b (Å)	93.1	93.2	93.1
c (Å)	73.8	73.9	73.9
R_{sym}[b]	6.7	3.8	5.5
Bragg resolution limit (Å)	1.90	1.90	1.85
no. of unique reflections	20666	21817	26171
av data redundancy	4.6	2.5	3.9
completeness of data (%)	84.6	88.0	91.0
final R-factor[c] (%)	13.7	14.9	14.5
bond length rms deviation (Å)	0.015	0.014	0.015
bond angle rms deviation (deg)	3.0	2.9	3.0
thermal/parameter correlation (Å^2)	5.0	5.0	5.0

[a] The previously reported crystal structure of the ecDHFR•MTX complex (Bolin, et al., 1982) belongs to space group $P6_1$ with two molecules per asymmetric unit; $a = b = 93.1$ Å and $c = 73.9$ Å. All three of the above binary crystal complexes are isomorphous with the ecDHFR•MTX binary complex. [b] $R_{sym} = \sum_{hkl}[\sum_i|\bar{I} - I_i|/\sum_i I_i]$. [c] R-factor $= \sum_{hkl}|F_o - F_c|/\sum_{hkl}F_o$.

Preparation of DHFR Binary Complex Crystals. 5dfol was a kind gift from Dr. John Montgomery of Southern Research Institute (Birmingham, AL). Eli Lilly & Co. (Indianapolis, IN) supplied the ddTHF (6*R* configuration to mimic natural THF). Folate was obtained from Sigma Chemical Co. (St. Louis, MO). All crystallizations were done at 4 °C by vapor diffusion against ethanol using the hanging-drop method. Protein solutions for crystallization were prepared by mixing 50 μL of the DHFR−ligand complex with 6.25 μL each of freshly prepared 0.5 M L-histidine hydrochloride, pH 6.8, and 0.5 M calcium acetate (Bolin et al., 1982). Reservoir solution was made up of 0.1 M Tris, pH 7.0, and 15%−25% ethanol. Droplet volumes were typically 5 μL, while reservoir volumes were 1.0 mL. Protein droplets were set on siliconized glass cover slips and then inverted onto the reservoir solution-filled wells of a 24-well Linbro tray (Flow Laboratories, Inc., McLean, VA), whose openings have been previously wiped thoroughly with vacuum oil (Apiezon Products Ltd., London, England). The trays were incubated in the dark at 4 °C and left undisturbed for 3−5 weeks, after which time large, well-diffracting crystals were observed.

Data Collection. Crystals were mounted at 4 °C in siliconized 1.0−1.5-mm diameter glass capillary tubes (Mark-Röhrschen, West Berlin, Germany), approximately 5 mL of mother liquor was placed in the top end and a similar amount of vacuum oil in the bottom end, and both ends were sealed with paraffin wax. Crystallographic data were collected at 4 °C on a Mark III Xuong−Hamlin multiwire area detector (Xuong et al., 1985; Hamlin, 1985). Complete data dets were collected from a single crystal for each complex. Table 1 summarizes the statistics for all data collections. R_{sym} is a measure of agreement among symmetry-related reflections. Data were reduced using a set of locally developed computer programs (Anderson, 1987).

Crystallographic Structure Refinement. The crystal structures of the three DHFR binary complexes were determined by difference Fourier methods. We first deleted atomic coordinates corresponding to MTX from the file of the previously published ecDHFR•MTX binary complex (Brookhaven PDB file name 4DFR) and used this ligandless coordinate set as the trial structure. All refinements were carried out with version 4A of the TNT refinement package

(Tronrud et al., 1987). After several cycles of refinement to reduce the *R*-factor to approximately 20%, $F_o - F_c$, α_{calc} difference maps were calculated and examined on a Silicon Graphics IRIS with the aid of the molecular graphics program TOM. Upon inspection of the active site, strong positive electron density was seen in the shape of the appropriate ligand. The ligand was then modeled into the difference density and the refinement process resumed. Adjustable parameters included molecular geometry as well as individual atomic *B*-factors. All atoms with *B*-factors of 100 Å^2 or greater were deleted, and water molecules were modeled into residual positive electron density peaks of reasonable magnitude, shape, and position (>3σ, roughly spherical, and 2.3–3.3 Å from a potential hydrogen-bonding group). Table 1 summarizes statistics pertaining to the refinement process. Coordinates of the 5dfol, folate, and ddTHF complexes have been deposited in the Brookhaven Protein Data Bank; their PDB file names are 1DYH, 1DYI, and 1DYJ, respectively.

Pairwise Comparisons of Refined Structures. Refinement results were analyzed by making pairwise comparisons among the above three complex structures and the previously reported MTX complex (Bolin et al., 1982). Least-squares superimposition of α-carbon coordinates for each pair was followed by computation of distance between corresponding atoms. Essentially identical results were obtained when the comparisons were performed with atom coordinates prior to least-squares superimposition, showing that the structures are indeed isomorphous.

An important quality control issue underlies such comparisons; it is usually taken for granted but must be addressed. To illustrate, suppose independent X-ray data sets are collected on two protein crystal specimens of identically the same structure. Then separate refinements are carried out. One expects, of course, to obtain slightly different coordinates, but in reality the two structures are actually identical and the "differences" are in fact due to random errors in data and refinement. To what extent is this happening in the comparisons reported here? To examine this question, we rely on the integrity of the $F_o - F_o$ map, meaning that random errors *in the data* should not, by and large, result in a map containing intelligible features. Then, to the degree that a standard least-squares refinement produces atomic coordinate shifts that are consistent with the $F_o - F_o$ map, the latter should resemble the corresponding $F_c - F_c$ map calculated from the two sets of refined coordinates. It was comforting that in each case the observed peaks and valleys in the $F_o - F_o$ maps agreed quite well with those in the calculated $F_c - F_c$ maps. An example is shown in Figure 2, which compares a portion of the F_o(folate) $- F_o$(ddTHF) and the F_c(folate) $- F_c$(ddTHF) maps in the vicinity of the ligand.

RESULTS AND DISCUSSION

The crystal structures reported here contain two molecules per asymmetric unit, in space group $P6_1$. We term them molecule A and molecule B. The mean uncertainty in atomic positions as calculated by the method of Luzzati (1952) is 0.2 Å for all three binary complexes.

B-Factor Profiles and Atomic Position Errors. The *B*-factor profiles of the α-carbon atoms of the folate, 5dfol, and ddTHF binary complexes, for both molecules A and B of the asymmetric unit, are very similar to those of the previously reported MTX binary complex. Each is characterized by six regions of high *B*-factor: residues 66–70 and 128–131 (*B*-factors 70–80 Å^2), residues 71–88 and 119–122 (*B*-factors 50–55 Å^2), and residues 48–52 and 104–108 (*B*-factors 30–40 Å^2). All are surface loops and are therefore expected to possess appreciable flexibility. The Met-20 loop (residues 9–23) is ordered in all three binary complexes, as it is in the MTX complex, with *B*-factors of 10–30 Å^2.

The *B*-factors of the ligand atoms are similarly distributed but are generally higher than for MTX in that complex, with values of 75–90 Å^2 for CG and the γ-carboxyl group of the glutamate moiety in the three complexes as compared with 45–50 Å^2 for MTX. In molecule B of the folate and ddTHF complex, in fact, these atoms are so disordered that they were deleted from the coordinate set. These observations may correlate with the fact that MTX is much more tightly bound than folate, 5dfol, or ddTHF.

Owing to weakness or invisibility of the relevant electron density due to disorder or thermal motion, a number of side-chain atoms have been deleted: in the folate complex, Cδ, Cγ, Nε2, and Oε1 of Gln-108 in molecule A and Cδ, Oε1, and Nε2 of Gln-318 in molecule B; in the ddTHF complex, Cδ, Cγ, Nε2, and Oε1 of Gln-108 and Cβ, Cδ, and Cγ of Pro-130 in molecule A and Cδ, Cγ, Oε1, and Nε2 of Gln-318 in molecule B. In the 5dfol complex, on the other hand, no side-chain atoms were omitted. In all three complexes, side-chain atoms originally omitted from the MTX complex structure remained invisible and were not reintroduced.

General Features of Ligand Conformations. To systematically examine any differences in conformation among the four ligands, we have made pairwise comparisons by superimposing each with the others.

Comparing folate and 5dfol, we find very little difference; their pteridine rings are almost perfectly coincident, and the same is true of the pABA rings and their glutamate residues (Figure 3, panel A). Thus there is no detectable in-plane rotation between their respective pteridine rings that might suggest differential hydrogen bonding of these two ligands. We will discuss the implications of this important finding in a latter section. The largest of the apparent positional differences, which may not be significant, are concentrated mainly within the pABG moiety. First, the dihedral angle between the pteridine and pABA rings seems to be about 4° larger for the 5dfol ligand than for folate. Second, their respective glutamate atoms O, N, CA, and CB differ in position by about 0.2 Å. It may therefore be concluded that the folate and 5dfol ligands, as bound to the enzyme, are nearly identical in conformation and orientation.

In the case of MTX as compared with either folate or 5dfol, it is readily apparent that its pteridine ring is rotated by 180° ("flipped") about an axis approximately collinear with a line through N5 and NA2 (Figure 3, panel B), consistent with previous results (Bolin et al., 1982; Bystroff et al., 1990). Moreover, the pABG moiety of MTX is translated upward by about 1.0 Å along the length of the pABA binding crevice. This translation seems related to the altered position of the pteridine ring which places C6 of MTX 1.7 Å closer to the pABG binding site. Also, while their pABA rings are almost coplanar, there is a relative in-plane rotation of 5° due to the flipped orientation of the MTX pteridine ring.

Turning next to a comparison between MTX and ddTHF, we observe that the pteridine rings of MTX and ddTHF form a dihedral angle of about 30°, with their respective NA4,

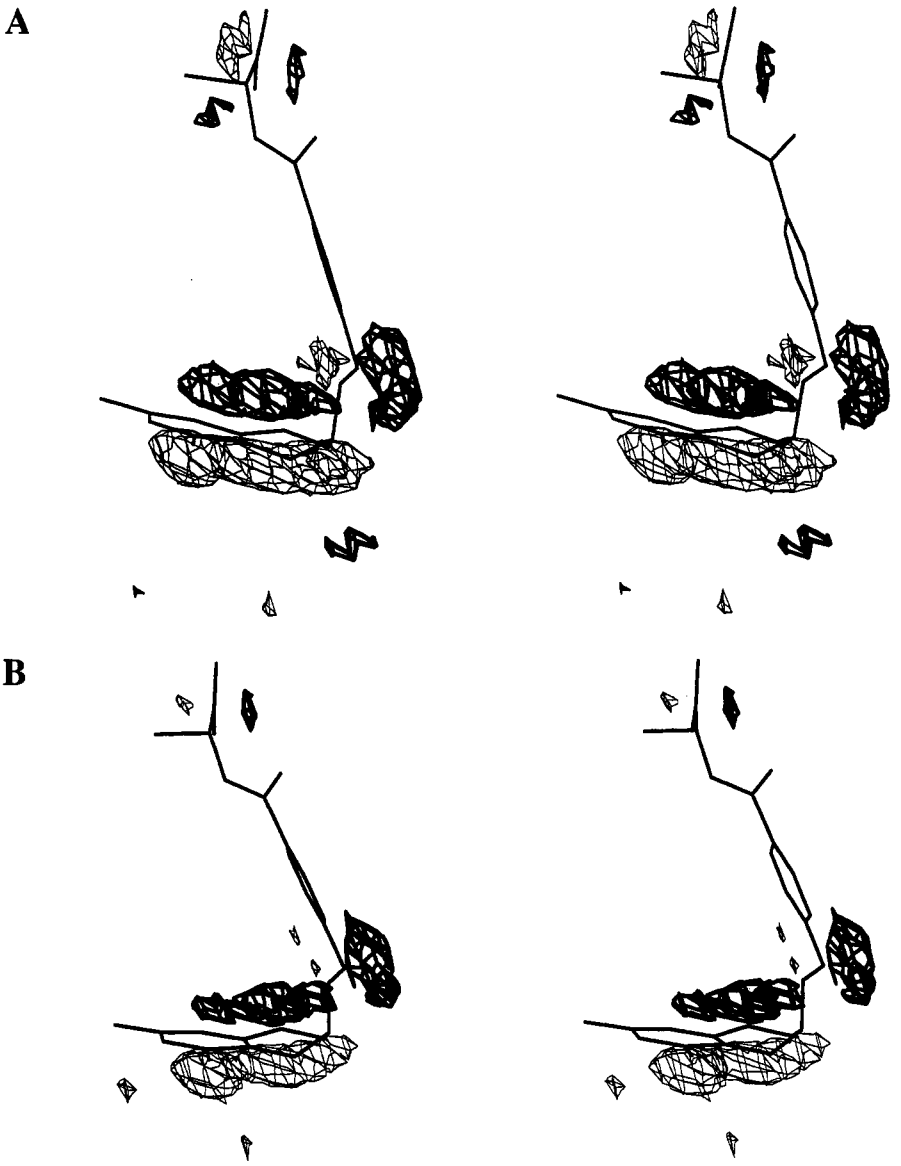

FIGURE 2: Comparison of a portion of the F_o(folate) − F_o(ddTHF) map (panel A) with the F_c(folate) − F_c(ddTHF) map (panel B), showing the electron density difference in the neighborhood of the ligand ddTHF, molecule B. Map contours are at approximately +4.5σ (heavy lines) and −4.5σ (thin lines).

N3, NA2 and N8, N1, C2 edges in common (Figure 3, panel C). The pABG moiety of MTX is also translated upward relative to that of ddTHF but only by about 0.5 Å, significantly less than observed in the comparison with folate or 5dfol. Additionally, the pABA rings of MTX and ddTHF are rotated with respect to each other by approximately 8°, apparently due to the reverse orientations of their respective pteridine rings. As in the previous case, the N10-bound methyl group of MTX is directed away from the pteridine moieties.

Comparison of ddTHF with either folate or 5dfol (Figure 3, panel D) reveals dramatic differences. The most obvious are at C6 and neighboring atoms. Whereas N5, C6, and C7 are coplanar with the rest of the pteridine ring in folate and 5dfol, the equivalent atoms are pyramidalized or "puckered" in ddTHF, consistent with the change in hybridization from sp^2 to sp^3 upon reduction of the N5−C6 bond. The reduced pyridine portion of the ring system may be described as a half-chair with C6 out of the plane. This puckering has long-range effects on the binding geometry of both the "pteridine" ring and the pABG moiety. The entire pteridine ring of ddTHF is slightly below that of folate or 5dfol, placing C5 and C7 closer to the nicotinamide binding site by 1.2 and 0.8 Å, respectively. The combination of displacement and puckering leaves C6 slightly above C5 and C7 but still closer to the nicotinamide binding pocket than in folate or 5dfol. Further, the pteridine rings of folate and ddTHF are tilted with respect to one another at a dihedral angle of about 25°, with their N8, N1, NA2 edges more or less coincident. The pABG moiety of ddTHF is translated upward, in the same direction as that of MTX, but by 0.5 Å instead of 1.0 Å. Accommodating this movement, pyramidalization at C6 alters the direction of the C6−C9 bond of ddTHF, rotating it 50° toward the pABG binding site relative to that of folate.

Detection of a Water Molecule Hydrogen Bonded to Pteridine O4 and N5 of Folate. Close examination of the electron density maps reveals that two to four water molecules are usually within 3.7 Å of the O4 atom of the folate, 5dfol, and ddTHF complexes. One, an invariant water molecule close to or hydrogen bonded to Oδ2 of Asp-27, Nε1 of Trp-22, and O4 of the pteridine ring (water-403 in molecule A and water-603 in molecule B), is observed in all crystal structures of ecDHFR with bound pteridine ligands. A mechanistic model of protonation at N5 (Bystroff

et al., 1990; Brown & Kraut, 1992) includes this water molecule as part of a proton relay system. However, recent findings (Blakley et al., 1993; Chen et al., 1994) cast doubt on its role, which therefore may be only pteridine ring binding rather than proton transfer. In any event, we do see the same water molecule in all three binary complexes.

We also find a few other water molecules in the neighborhood of N5 of the three ligands. In the folate complex water-567 in molecule A and water-805 in molecule B (see Figure 4) are both hydrogen bonded to the pteridine O4 and N5 at 2.9 and 3.2 Å, respectively. This water molecule (in both molecules A and B) is connected by a series of four to five other water molecules to the protein exterior. In the 5dfol and the ddTHF complexes, on the other hand, we fail to detect a similarly positioned water in either molecule of asymmetric unit. This clear distinction is almost certainly due to the C5 to N5 substitution in both the 5dfol and ddTHF ligands. We believe these are important observations for understandng the mechanism of N5 protonation.

In the introduction we described current models for the mechanism of protonation at N5. These models, regardless of other details, postulate the transient existence of a water molecule hydrogen bonded to O4 and N5 which ultimately delivers a proton to N5. The presence of just such a water molecule in the crystal structure of the ecDHFR•folate complex reported here strongly supports such an idea. This water molecule is thought to be present only transiently because it is not seen in structures where the Met-20 loop is closed down onto the pteridine binding site. In fact, a similarly positioned water molecule had previously been observed in the clDHFR complex with biopterin (McTigue et al., 1992). In that case it was argued that hydrogen bonding to the dihydroxyisopropyl tail of biopterin is necessary to hold the transient water molecule in place. The present result demonstrates that such ordering by the dihydroxy group is not necessary, at least in the *E. coli* enzyme. However, in the ecDHFR•folate•$NADP^+$ ternary complex (space group $P3_221$; Bystroff et al., 1990), no water was seen hydrogen bonded to either pteridine O4 or N5. This may correlate with our recent observation that, in other $P3_221$ DHFR crystal structures, the Met-20 loop is always ordered and closed over the pteridine binding site, apparently excluding any water molecule. On the other hand, in a new ecDHFR•folate•$NADP^+$ ternary complex crystal, space group *C*2, such a transient water molecule *is* observed hydrogen bonded to pteridine O4 and close to N5 (M. R. Sawaya, in preparation). Apparently, differences in crystal packing affect the Met-20 loop conformation, which is in turn sufficient to determine whether or not this transient water molecule occurs in the crystal structure.

Interaction of the Pteridine Ring with Neighboring Enzyme Atoms. The C7−N8 bond of DHF is reduced, whereas that of folate is not; therefore, an additional hydrogen is available at N8 of DHF for hydrogen bonding to a nearby acceptor. If folate or 5dfol were protonated at N8, they should also be able to hydrogen bond to the same acceptor. Ile-5(O) the backbone carbonyl oxygen at Ile-5, is such a potential hydrogen bond acceptor close to N8. The previously determined structure of ecDHFR•folate•$NADP^+$ (Bystroff et al., 1990) revealed that the N8 to Ile-5(O) distance is 3.6 Å, indicating the absence of hydrogen bonding between N8 and Ile-5(O). However, a closer approach of 2.8−3.0 Å, as required for hydrogen bonding, may be attained in two ways: the pteridine ring can undergo an in-plane rotation, or the peptide bond between Ile-5 and Ala-6 can twist by about 22°, suitably repositioning Ile-5(O). This latter adjustment is precisely what happens to the equivalent peptide bond (Ile-7/Val-8) in the huDHFR•5dfol complex (Davies et al., 1990). On this basis it was proposed that 5dfol is protonated at N8 when bound to huDHFR and thus can hydrogen bond with Ile-7(O). Folate itself, with a much lower pK_a at N8, cannot perform this feat except, presumably, in the protonated transition state for folate reduction. Williams and Morrison (1992) later showed that 5dfol, when bound to huDHFR, is indeed protonated, with its pK_a elevated to 10 from a normal value of 4.

In the present *E. coli* DHFR complexes, the N8 to Ile-5(O) distances are 3.5, 3.4, and 3.2 Å for folate, 5dfol, and ddTHF, respectively, and no twisting of the Ile-5/Ala-6 peptide bond is evident, indicating the absence of hydrogen bonding between N8 and Ile-5(O) in all three cases. More specifically, we note that the N8 to Ile-5(O) distance in the 5dfol complex of 3.4 Å is not significantly different from that of folate. We conclude, therefore, that N8 of 5dfol bound to *E. coli* DHFR is unprotonated, in contrast to the case of huDHFR. Thus, perhaps because of the greater flexibility of its backbone chain at Ile-7/Val-8, huDHFR appears to have a greater tendency to favor protonation at the N8 position than does ecDHFR. Since protonation of N8 is expected in the transition state for folate reduction, this property may help to explain why the vertebrate enzyme in much better than the bacterial enzyme at catalyzing the reduction of folate to DHF. However, we are unable to attribute the proposed difference in flexibility of the huDHFR and ecDHFR in their corresponding Ile-7/Val-8 and Ile-5/Ala-6 regions to any particular structural features; both chain segments are part of the βA strand, and there are no obvious distinctions between them.

In the case of ddTHF, a marginally decreased N8 to Ile-5(O) distance of 3.2 Å is almost certainly due to puckering of the pteridine ring rather than to an in-plane rotation toward Ile-5(O) or twisting of the Ile-5/Ala-6 peptide plane toward N8.

The pteridine binding site of ecDHFR is predominantly hydrophobic except for a single ionizable residue, Asp-27. As discussed earlier, this residue may be involved in protonation at N5, which is presumably required for the subsequent hydride transfer from the cofactor to C6. Another function of Asp-27, however, is to hold the pteridine ring in place by forming a pair of hydrogen bonds between its Oδ1 and Oδ2 atoms and the pteridine's NA2 and N3. The degree of dissymmetry in the geometries of these two hydrogen bonds may thus be taken as an indicator of the degree of strain in the interaction between the pteridine ring and the Asp-27 side chain. In the ecDHFR•folate•$NADP^+$ complex these hydrogen bond lengths are 2.6 and 3.2 Å, respectively (Bystroff et al., 1990); the significant difference of 0.6 Å indicates an appreciably strained interaction. In the present binary complexes, however, we cannot detect any appreciable dissymmetry between these two hydrogen bonds: in the folate complex, the NA2−Oδ1 distance is 2.9 Å and the N3−Oδ2 distance is 2.7 Å; in the 5dfol complex, the corresponding distances are 2.8 and 2.7 Å; and in the ddTHF complex, they are 2.9 and 2.7 Å. In the MTX complex, although one of the H-bonding groups in the pteridine ring is different because of the ring's reverse orientation, the corresponding H-bond lengths are similarly symmetrical: the NA2−Oδ1 distance is 2.8 Å and the N1−Oδ2 distance is

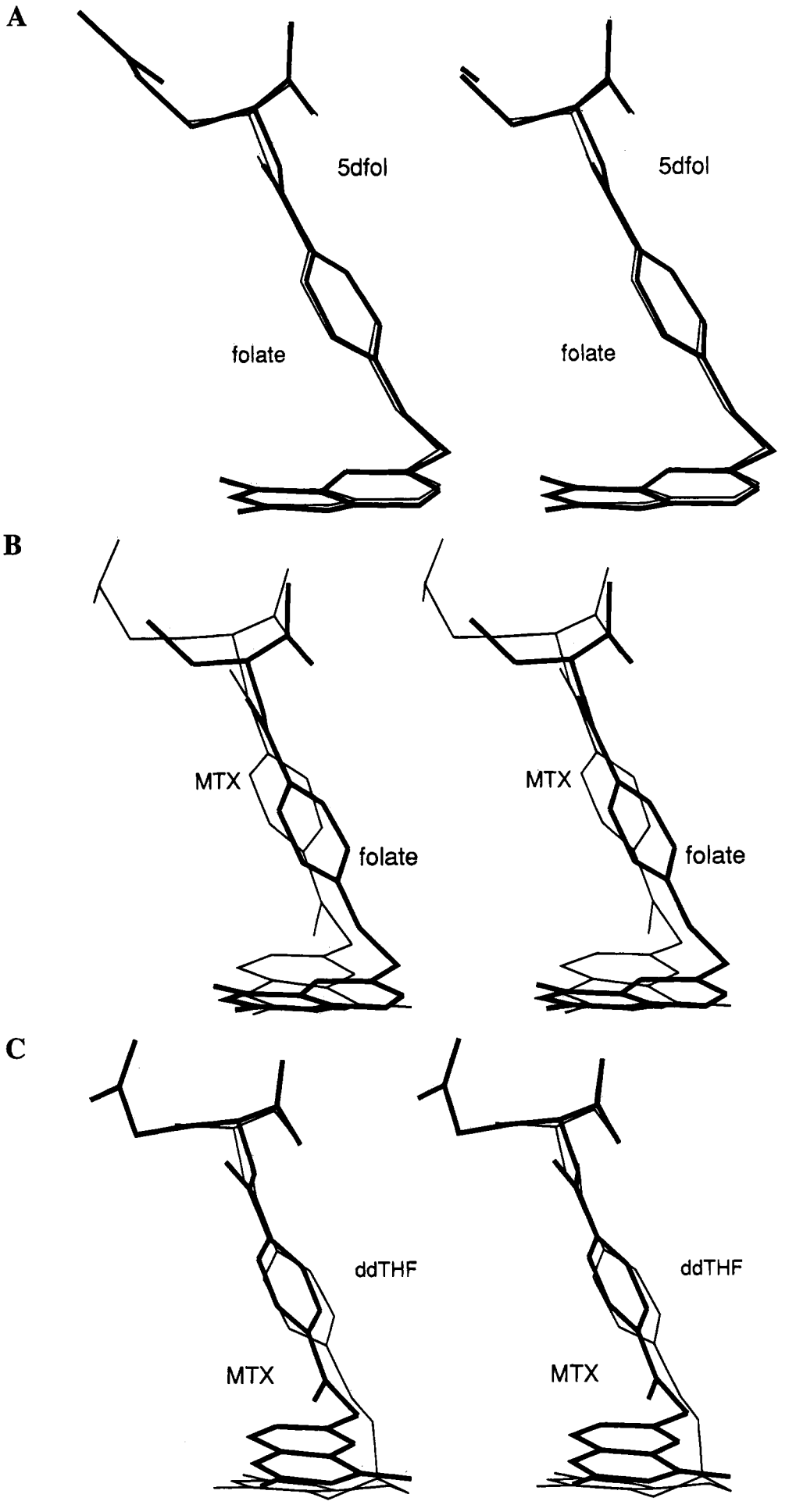
A
5dfol
folate
5dfol
folate
B
MTX
folate
MTX
folate
C
ddTHF
MTX
ddTHF
MTX

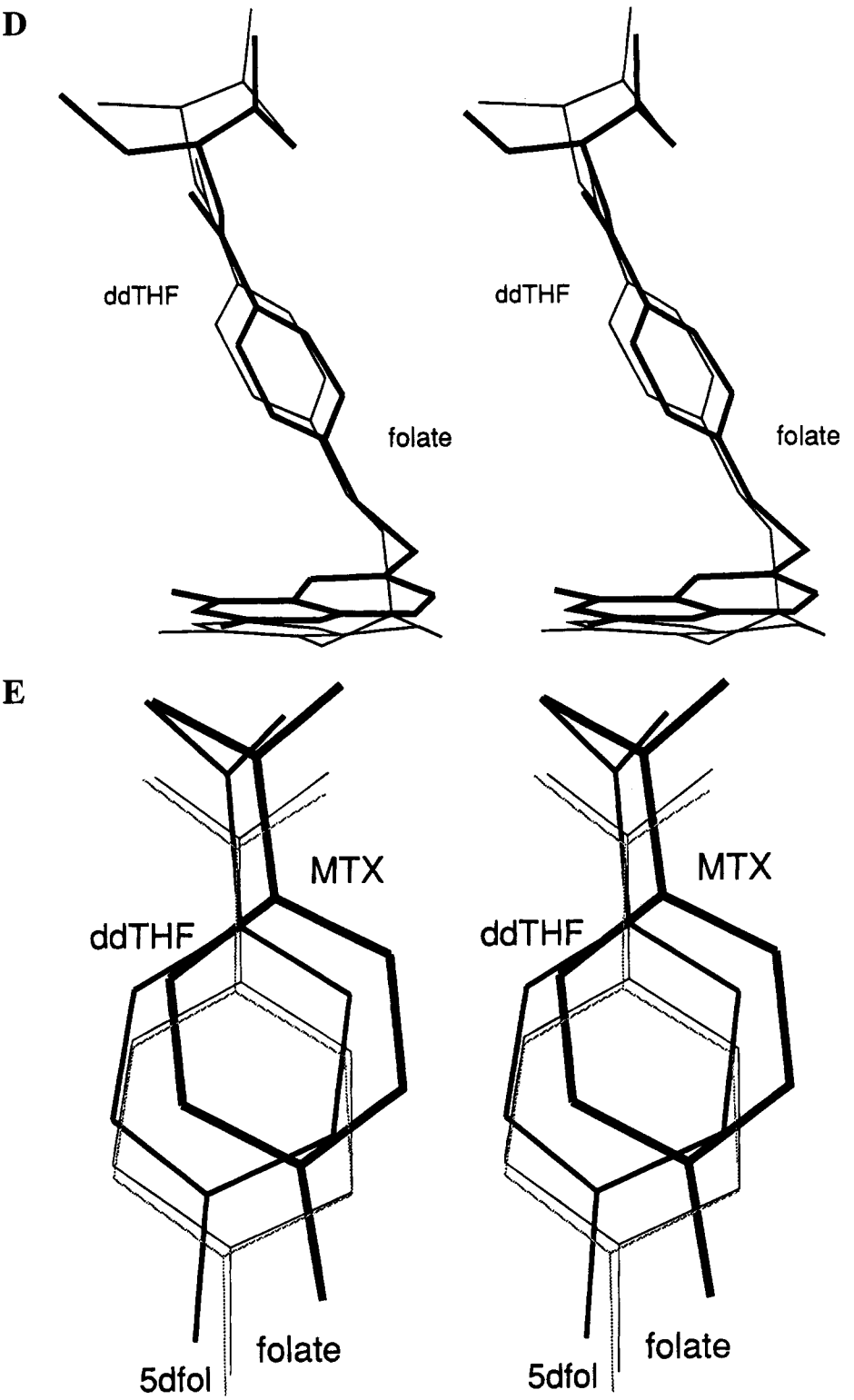

FIGURE 3: Pairwise comparisons among the ligands in the four binary complexes; each depicts molecule B of the asymmetric unit. Panels: (A) 5dfol (thick lines) and folate (thin line); (B) folate (thick lines) and MTX (thin lines); (C) MTX (thick lines) and ddTHF (thin lines); (D) folate (thick lines) and ddTHF (thin lines). Panel E shows a superposition of the four complexes, focusing on their pABA rings: thick lines, MTX; medium lines, ddTHF; thin lines, folate; broken lines, 5dfol. In each comparison, refined atom coordinates were superimposed using a facility of the program INSIGHT II.

2.6 Å. These observations suggest that the presence of the cofactor in the ternary complex may impart a degree of strain in substrate binding, perhaps promoting the transformation of the Michaelis–Menten complex into the transition state. This hypothesis is supported by the existing kinetic data. The rate constant for dissociation of DHF from the ecDHFR·DHF·NADPH ternary complex is twice that from the ecDHFR·DHF binary complex; and, since the two association rate constants are equal, the dissociation constant is also twice as large for the ternary complex as compared with that for the binary complex (Fierke et al., 1987).

In Search of the Transition-State Geometry. A basic tenet of enzymology holds that enzyme catalysis occurs because the enzyme binds the transition state for the reaction much more strongly than it does the reactants [for a discussion, see Kraut (1988)]. Thus, one important aspect of the

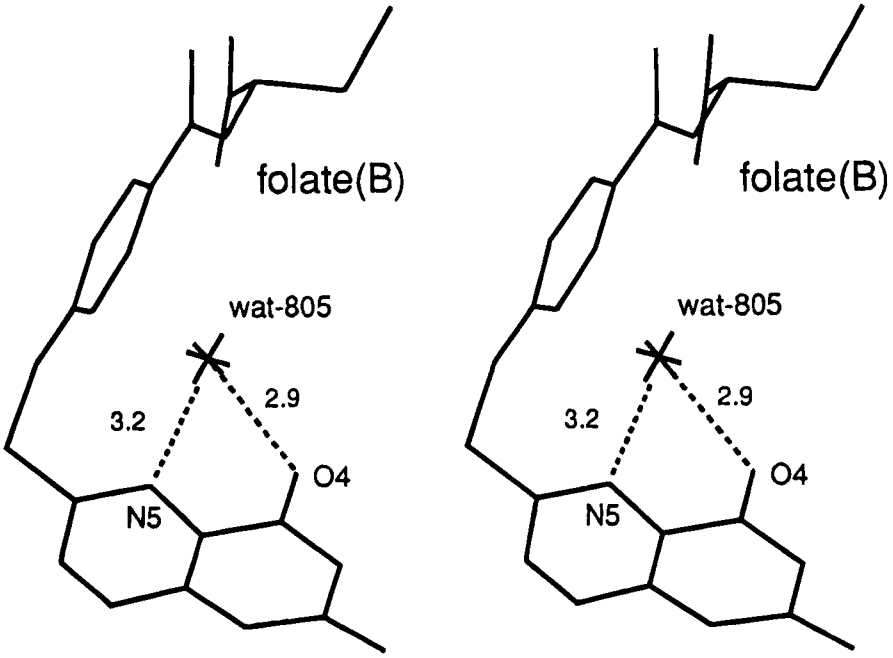

FIGURE 4: Bound water molecule in the folate complex (water-567 in molecule A and water-805 in molecule B) believed to be involved in protonation of pteridine N5. The structure and distances (in Å) shown are from molecule B of the asymmetric unit. The water is shown hydrogen bonded to atoms O4 and N5 of the pteridine ring. Corresponding hydrogen bond distances in molecule A are identical.

transition state for hydride transfer is that the hydride donor and acceptor atoms must be separated by a distance that is less than the sum of van der Waals radii but greater than the sum of two covalent C−H bonds. One expects, therefore, that DHFR will preferentially bind cofactor and substrate in such a way as to make the distance between C4 of the nicotinamide and C6 of the pteridine ring appropriate for the transition state. Recently, the crystal structure of the binary ecDHFR•NADPH complex has been solved and refined in this laboratory (space group $P3_221$; M. R. Sawaya, in preparation; coordinates have been deposited in the Brookhaven Protein Data Bank under the file name 1DRH). To our knowledge this is the first ecDHFR−cofactor crystal structure (i.e., without a simultaneously bound substrate or analog) in which the nicotinamide ring of the cofactor is sufficiently ordered that it can be seen in the electron density map. Its importance in the present context is that it allows us to superimpose the *separately bound* cofactor and folate ligands, which in turn should reveal the geometry favored by the enzyme for the approach between the nicotinamide ring of the cofactor and the pteridine ring of substrate; that is, it allows us to investigate the transition-state geometry favored by *E. coli* DHFR.

For this purpose we employed the superposition program OVERLAY, which performs a least-squares fitting of two protein structures on the basis of their respective α-carbon positions. OVERLAY is among the programs included in the crystallographic software package, TNT. When the NADPH-containing holoenzyme structure was superimposed on both molecules A and B of the folate, 5dfol, and ddTHF complexes, the rms Cα deviations were all between 0.8 and 1.0 Å. We then calculated the closest approach between the nicotinamide and pteridine rings (see Figure 5). In all cases the closest approach occurred between the hydride donor, nicotinamide C4, and the pteridine C7. The C4−C7 distances (average between molecules A and B) for folate, 5dfol, and ddTHF complexes are 2.6, 2.6, and 1.8 Å, respectively. However, the nicotinamide C4 to pteridine C6 distances (average between molecules A and B) are only 0.3−0.4 Å greater; in the folate, 5dfol, and ddTHF complexes they are 2.9, 2.8, and 2.2 Å, respectively. The result of this overlap of pteridine and nicotinamide binding sites is also evident in the close contacts observed in ground-state ternary complexes. C4−C7 distances of 3.2, 3.3, and 3.2 Å occur in ecDHFR•folate•$NADP^+$ complexes in space groups $P3_221$, $P2_1$, and $C2$. In fact, close contact with the rigidly fixed nicotinamide ring rotates the pterin ring so that the pyrazine portion is pushed away by 0.4−0.6 Å (Sawaya, 1994).

Davies et al. (1990) did a similar least-squares superimposition of the huDHFR•folate binary complex (space group $P1$) and the clDHFR•NADPH holoenzyme complex (space group $C2$), with similar results. In that case, representative of the vertebrate DHFR's, it was also found that the closest approach of substrate and cofactor occurred between the nicotinamide C4 and the pteridine C7, at 2.4 Å, while the nicotinamide C4 to pteridine C6 distance was 2.6 Å. Hydride transfer is believed, on the basis of theoretical calculations, to occur *via* a bent geometry with an optimal distance between donor and acceptor atoms of 2.6 Å (Wu & Houk, 1987a,b). Thus it seems quite clear that DHFR is "designed" to bind the substrate and cofactor with a sub-van der Waals contact that is optimal for hydride transfer.

The results of the above superimpositions with ddTHF, however, require further comment. We note that the closest approach distance between ddTHF and NADPH, 1.8 Å, is exceptionally short. We believe that this highly unfavorable contact plays an important role in product release and will address the issue in a later section.

Another important aspect of the transition-state geometry for hydride transfer is that both C4 of the nicotinamide and C6 of the pteridine ring should be somewhat pyramidalized. Inspection of the complexes reported here shows that pyramidalization at C6 of the pteridine ring may be induced by several features of the local structure. Among the most notable is an unfavorably close approach between C6 and C15 of the pABA ring above it, which tends to push C6 down toward the cofactor's nicotinamide ring. We measured the C6−C15 distance in the binary complex structures, and

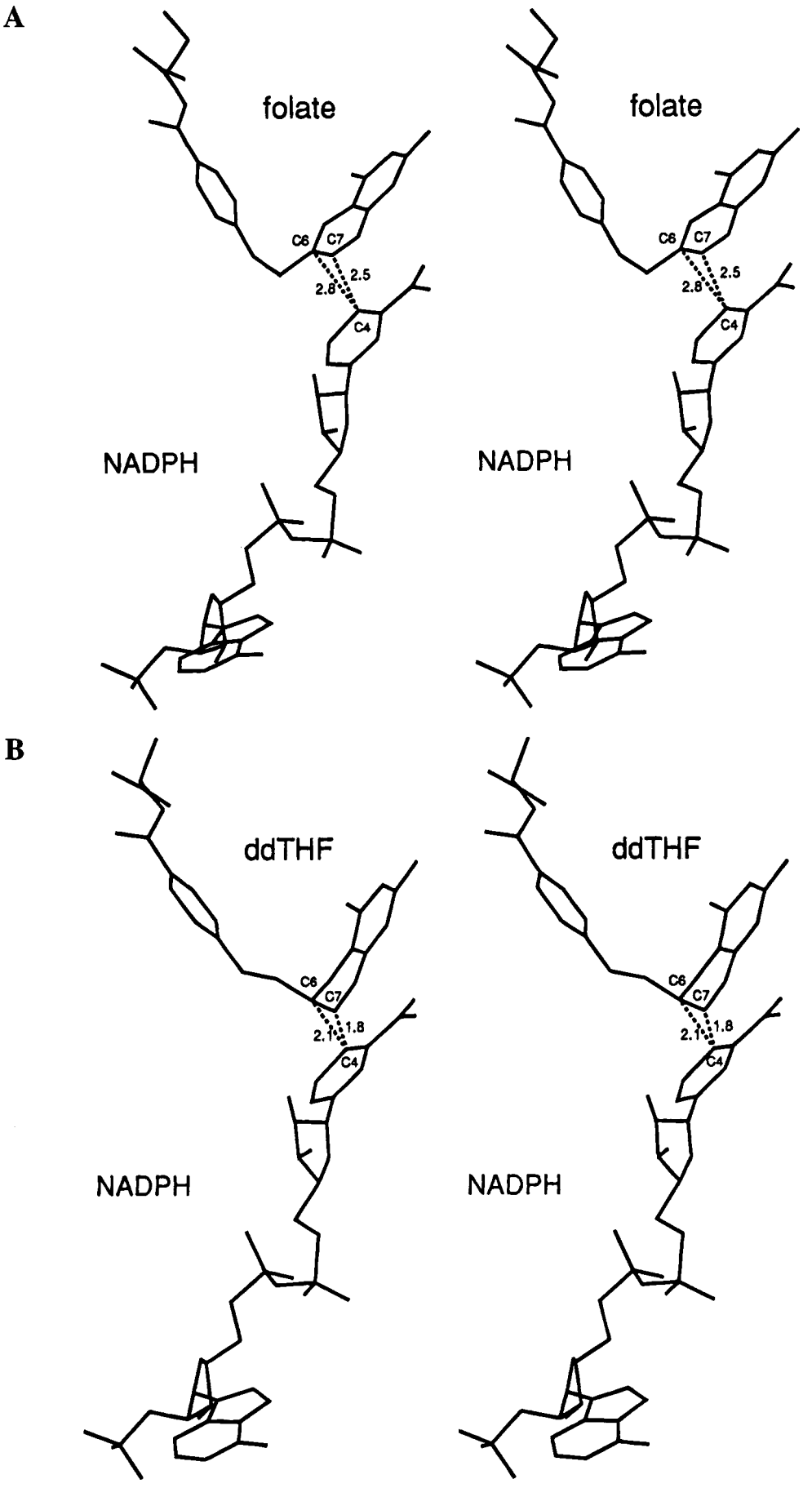

FIGURE 5: Least-squares superimposition of the NADPH holoenzyme structure ($P3_221$; M. R. Sawaya, in preparation) with each of the three binary complex structures. Molecule B of the asymmetric unit is shown in each case. Panels: (A) folate; (B) ddTHF. All least-squares superimpositions were based on Cα carbon coordinates. Distances (in Å) between C4 of the cofactor and C6 and C7 of the pteridine ring are indicated. The corresponding distances for the 5dfol complex are C4−C6, 2.7 Å; and C4−C7, 2.5 Å.

the values obtained for folate, 5dfol, and ddTHF are 3.2, 3.2, and 4.3 Å, respectively. Since van der Waals contact is normally 3.5−3.8 Å, we surmise that appreciable steric strain must be generated by this contact in folate and 5dfol but not in ddTHF. Presumably, the nonplanarity of the pteridine ring of ddTHF relieves the close contact between C6 and C15. These observations suggest that, as would be anticipated, ecDHFR preferentially binds a transition-state conformation that more closely resembles ddTHF, and therefore the product THF, than it does folate or 5dfol. It seems reasonable to surmise that the pteridine ring conformation in the transition state is somewhere between that of DHF and THF.

Positioning of the pABG Moiety. Evidently the *p*-aminobenzoyl glutamate tail of the substrate, although not a direct participant in the hydride-transfer reaction, must play some role in the catalytic mechanism. Thus molecules containing the dihydropterin ring but not the pABG tail, like dihydrobiopterin and 6-methyldihydropterin, are poor substrates for DHFR. The reason for this is not yet known, but in any case the pABG must do more to enhance binding of the transition state than of the ground state. When bound to the enzyme, the pABA ring is sandwiched between the αB and αC helices, with Cδ2 of Leu-28 in the αB helix and Cγ1 of Ile-50 in the αC helix making the closest contacts. Comparing the ecDHFR•folate•$NADP^+$ ternary complex ($P3_221$) with the ecDHFR•MTX binary complex ($P6_1$), Bystroff et al. (1990) noted that the pABA ring of MTX is displaced by 1.3 Å relative to that of folate. It was suggested that the enzyme favors a pABA binding geometry closer to what is seen in the MTX complex and that a strained conformation, apparent in the case of bound folate, is relaxed in the transition state by pteridine ring puckering and relief of the close contact between C6 and C15 (Bystroff & Kraut, 1991). However, the ecDHFR•folate•$NADP^+$ and the ecDHFR•MTX structures being compared had been solved in different crystal packings ($P3_221$ and $P6_1$, respectively), and moreover, the first was a ternary complex while the second was a binary complex. Thus either or both of these factors might have been the actual cause of the pABA shift rather than any intrinsic propensity of the DHFR molecule to bind the pABA in one or the other precise position. Now, however, we have four ligands all in binary complexes and all in the same crystal packing, $P6_1$, and can ask whether there really is an appreciable difference in their pABA positions. It is gratifying to report that indeed there is, in essential agreement with the earlier finding (but see below) of Bystroff et al. (1990).

If we first determine the coordinates of the pABA ring centroids in each of the four complexes and then compute their mutual distances, we find, not surprisingly, that the pABA rings of folate and 5dfol are within 0.1 Å of each other and therefore may be considered coincident (see Figure 3A). In contrast, however, the pABA ring centroids of folate and MTX are translated by about 1.0 Å relative to one another (Figure 3B), those of ddTHF and MTX by 0.8 Å (Figure 3C), and those of ddTHF and folate by 0.6 Å (Figure 3D). Interestingly, the pABA ring of ddTHF is positioned approximately halfway between its location in folate and in MTX (Figure 3E). Displacement of the pABA ring of MTX or ddTHF relative to that of folate may best be described as an upward translation along the pABG binding crevice, with a small translational component toward the αB helix.

Note that Figure 3B is directly comparable to Figure 4 in Bystroff et al. (1990); however, it is evident that the latter depicts a somewhat different relative translation of the two pABA rings. In an effort to get to the bottom of this apparent discrepancy, we recalculated the comparison of Bystroff et al. (1990), this time using two different and more recent least-squares superposition programs, INSIGHT II (Biosym Technologies, San Diego, CA) and OVERLAY. Both resulting comparisons between bound folate and bound MTX (in different space groups) produced results closely resembling our present Figure 3B rather than Figure 4 of Bystroff et al. (1990). The reason for the discrepancy is unknown, but it is our impression that it might be due to a difference in the least-squares algorithm in the programs (Bystroff et al. used the program OVRLAP; Rossmann & Argos, 1975). In any case, all comparisons produced similar results.

We next compared interactions between the pABG moiety and the enzyme among the four complexes. No differences involving the glutamate were evident, but we did find some variation in the distances from the pABA rings to Leu-28(Cδ2) in the αB helix and to Ile-50(Cγ1) in the αC helix. In the folate and 5dfol complexes, the pABA ring centroids are closer to the αC helix than to the αB helix by about 0.3 and 0.7 Å, respectively, implying some degree of strain. In the MTX and ddTHF complexes, on the other hand, the pABA ring centroids are both equidistant from the two helices. The details are as follows: in the folate complex the pABA ring centroid is 4.3 Å from αB and 4.0 Å from αC, and in the 5dfol complex it is 4.5 Å from αB and 3.8 Å from αC. In the MTX complex the pABA ring centroid is 4.0 Å from αB and 4.1 Å from αC, and in the ddTHF complex, it is 4.2 Å from αB and 4.2 Å from αC. Note that although the differences are small, the distances given are averages for the two molecules of the respective asymmetric units and are therefore probably significant. Thus, the impression conveyed is that the folate and 5dfol ligands are in a somewhat strained conformation, while the ddTHF and MTX ligands are not.

From these observations it may be inferred that DHFR is designed to bind the pABA ring more nearly in a position characteristic of the MTX complex than of the folate complex, as was previously suggested by Bystroff et al. (1990, 1991). Perhaps this preference reflects a transition-state geometry in which the pABA ring is nestled between αB and αC, equidistant between the two, comfortably accommodating a suitably puckered pteridine ring. In the case of MTX, the more favorable binding position of the pABA ring is allowed because the 2,4-diaminopteridine ring is flipped over.

Finally, we may ask whether the above observations correlate with overall backbone movements, if any, of the enzyme. Bystroff and Kraut (1991) earlier proposed that ecDHFR is composed of two "domains"—in the sense of dynamical structures, rather than in the usual sense of folding units—namely, a major domain and a smaller adenosine binding domain connected by a short hinge section, between which lie the cofactor and substrate binding crevices. It was observed that binding of MTX to the apoenzyme results in a 6° relative rotation of these domains, resulting primarily in closure of the pABG binding crevice by some 2 Å. Do folate, 5dfol, and ddTHF induce a similar effect? To answer this question, we compared the enzyme conformations in the folate, 5dfol, ddTHF, and MTX complexes, as well as that of the apoenzyme, by visual analysis of their respective least-

squares superimposed backbone traces, as well as by calculating two-dimensional distance difference plots (Bystroff & Kraut, 1991). We found that indeed there is such a domain rotation and pABG binding crevice closure in the MTX complex, but in the folate, 5dfol, and ddTHF complexes the pABG crevices remain relatively open, all to a similar degree, but still slightly constricted as compared to the apoenzyme. We term these backbone chain conformations "closed" in the case of the MTX complex, "partially open" in the case of the other three complexes, and "fully open" in the case of the apoenzyme (Sawaya, 1994). A word of caution: the present "open" and "closed" designations are unrelated to the orientation of the Met-20 loop; rather, they pertain solely to the relative dispositions of the two domains of the enzyme, discussed earlier. Assuming that the DHFR conformation in the folate and 5dfol complexes more nearly resembles the Michaelis complex, MTX the transition state, and ddTHF the product complex, then these observations suggest that the enzyme undergoes domain closure during approach to the transition state and subsequently reopens after the products have formed.

A Structural Basis for Slow Product Release. The ecDHFR-catalyzed reaction is characterized by a slow, rate-limiting release of the product, THF, which is, however, stimulated to a significant extent by binding of a fresh molecule of NADPH (Fierke et al., 1987; Stone & Morrison, 1988; Morrison & Stone, 1988; Penner & Frieden, 1987). The relative "product stickiness" of THF is illustrated by its slow dissociation as compared with DHF from both the binary and ternary complexes. Specifically, DHF dissociates from the binary complex with the *E. coli* enzyme some 14 times faster than does THF, 20 s^{-1} as compared with 1.4 s^{-1} (Fierke et al., 1987); and similarly, though less dramatically, dissociation of DHF from either the $NADP^+$ or the NADPH ternary complex is about 3 times faster than dissociation of THF from the corresponding ternary complexes. Another distinctive characteristic of the ecDHFR-catalyzed reaction is that THF release is accelerated by binding of a new NADPH molecule. Thus dissociation of THF from the ecDHFR·THF·NADPH ternary complex is about 9 times faster than from the ecDHFR·THF complex, with rate contstants 12.5 and 1.4 s^{-1}, respectively (Fierke et al., 1987).

What is the structural basis for these observations? Although owing to the instability of DHF we do not yet have a crystal structure for DHFR with bound substrate, we are probably on safe ground arguing that the binding geometry of DHF will not be very different from that of folate of 5dfol. In any case, examining the interaction between the entrance to the catalytic site in ecDHFR and the ligands in all three of our present complexes, we find that the interaction between Trp-22(Nϵ1) and the pteridine O4 is the most clearly different among the three complexes. It is important to note here that while Trp-22 formally lies within the Met-20 loop, residues 9−23, it is not part of the mobile tongue-shaped "flap" roughly comprising six or seven residues, 15−21 (M. R. Sawaya and H. Lee, unpublished observations). Specifically, we find that the Nϵ1−O4 distance in the ddTHF complex of 4.9 Å is significantly shorter than in the folate and 5dfol complexes, which are 5.5 and 5.4 Å, respectively (Figure 6). Since there is no indication that the position of the Trp-22 side chain differs among the complexes, we conclude that puckering of the pteridine ring of ddTHF must bring O4 closer to Trp-22. Moreover, an ordered water molecule (water-403 in molecule A and water-603 in molecule B) bridging Trp-22(Nϵ1) and the pteridine O4 appears positioned to make more nearly ideal hydrogen bonds in the ddTHF complex than in the folate or 5dfol complexes. The same ordered water molecule, also hydrogen bonded to Asp-27, is observed in all pteridine-liganded DHFR structures determined so far. In the ddTHF complex the invariant water is within hydrogen-bonding distance of both Trp-22(Nϵ1) and pteridine O4, at 3.2 and 2.8 Å; moreover, the hydrogen bond angle at the water oxygen atom is an ideal 108°. Compare this geometry with the folate or 5dfol complexes, in which the water molecule is 3.4 or 3.5 Å from Trp-22-(Nϵ1) and 3.0 or 2.9 Å from pteridine O4, and the hydrogen bond angles at the water oxygen atom are 117° or 116°. Although the differences are small, they are perhaps significant since the distances and angles quoted are averages over two molecules in the asymmetric unit. We suggest, therefore, that owing to puckering of the reduced pteridine ring of ddTHF, and presumably of THF as well, if can make a more favorable interaction with Trp-22 via the conserved water molecule bridging Nϵ1 and O4. We suggest that this enhanced interaction could slow the dissociation of THF from the enzyme.

The involvement of Trp-22 in product release had been indicated previously by site-directed mutagenesis and kinetics studies (Warren et al., 1991). When Trp-22 in ecDHFR was replaced by either Phe or His, the rate of hydride transfer decreased by about 3-fold, while the rate of steady-state catalysis was elevated 3-fold. Deuterium isotope effects showed that hydride transfer became at least partially rate-limiting in both mutants. The interpretation offered was that THF release, which is limiting for the wild-type enzyme, has been substantially accelerated by the mutations. Unexpectedly, the crystal structure of the Phe-22 mutant (the His-22 mutant could not be crystallized) showed that the invariant water molecule (water-403 in molecule A and water-603 in molecule B) is still in place despite the mutation. In light of our present structural analysis the probable cause of the above increased THF release rate seems obvious: neither Phe-22 nor His-22 can form the critical H-bonded bridge with the invariant water molecule.

There may be an additional structural factor contributing to the low dissociation rate of THF, namely, the precise positioning of its pABA ring in the pABG binding crevice. As was fully discussed in the previous section, because the reduced pteridine ring of ddTHF is highly puckered, the binding position of its pABA ring approaches that of MTX more closely than do those of the folate or 5dfol; i.e., its pABA ring is translated upward somewhat, lying midway between folate's and MTX's (Figure 3E). Since the pABA rings of ddTHF and MTX are both equidistant from their flanking α helices, while that of folate is pushed to one side, we suggest that an MTX-like position for the pABA ring is more favorable energetically. Thus, this effect may also contribute to the slow release of THF from the enzyme−product complex.

These observations may be summarized as follows. In the folate and 5dfol complexes (and presumably in the DHF complex) the enzyme assumes a partially open conformation, while the pABA moiety is held unsymmetrically within the pABG crevice. In contrast, the closed conformation of the enzyme when MTX is bound and the unstrained positioning of its pABA moiety might contribute to the tight binding of

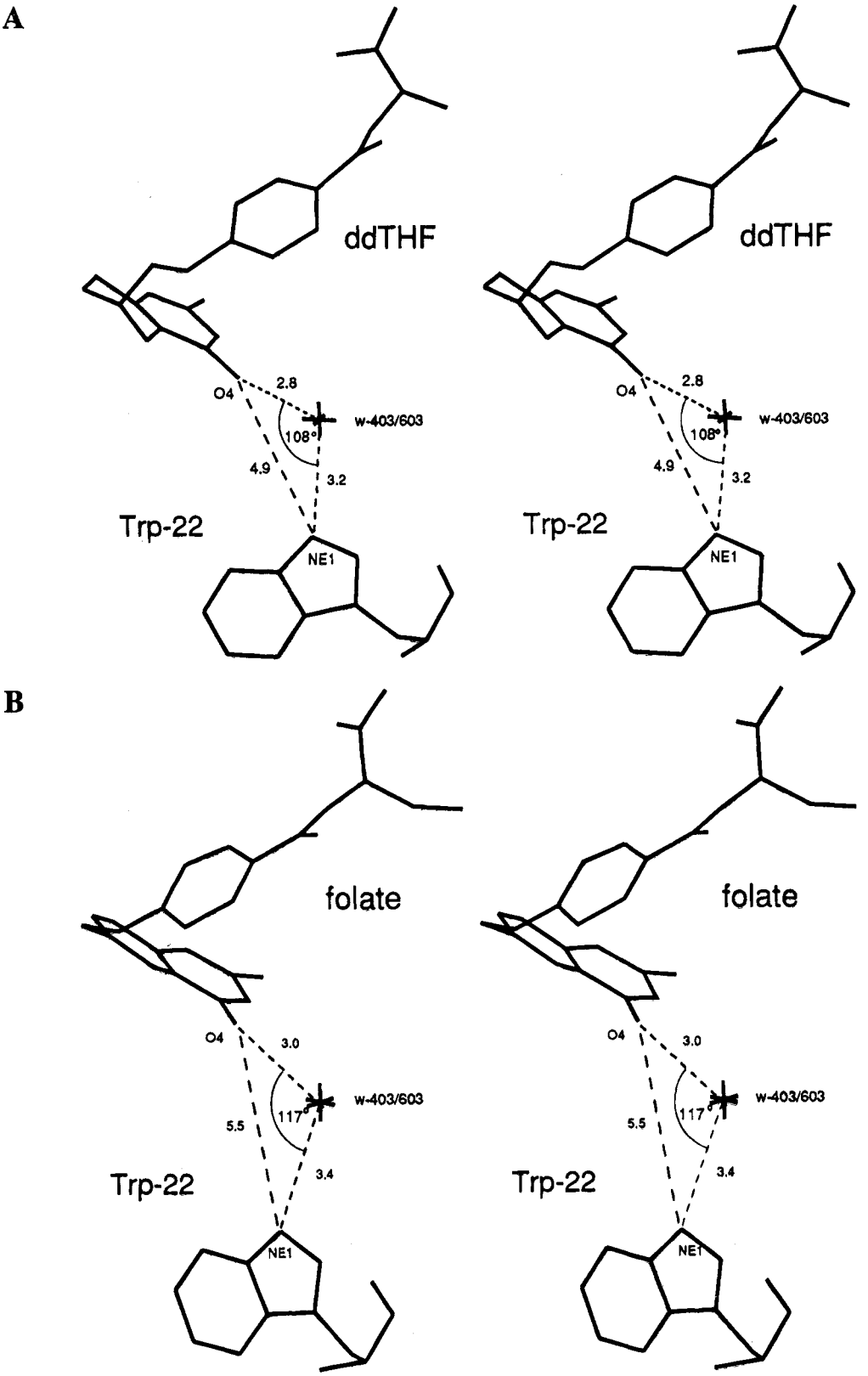

FIGURE 6: Ordered water molecule (water-403 in molecule A and water-603 in molecule B of the asymmetric unit) bridging pteridine O4 and Trp22(Nϵ1) in the ddTHF (panel A) and folate (panel B) complexes. Structures shown are actually molecule B of the asymmetric unit, but the distances (in Å) and angles indicated are the average values for the two molecules. For the 5dfol complex, which is essentially identical with the folate complex, the corresponding values are O4–Nϵ1, 5.4 Å; O4–water, 2.9 Å; Nϵ1–water, 3.5 Å; and O4–water–Nϵ1 angle, 116°. The water molecule is also hydrogen bonded to Oδ2 of Asp-27 (not shown).

MTX. Additionally, a water molecule bridging O4 of the pteridine ring and Trp-22(Nϵ1) is positioned in a less than optimal geometry for hydrogen bonding in the case of folate and 5dfol. In the ddTHF complex, it is evident that these particular ligand–enzyme interactions are intermediate between those of MTX and folate. The enzyme conformation is open, but the pABG moiety of ddTHF occupies a relatively unstrained position, halfway toward that of MTX, and the bridging water molecule makes better hydrogen bonds than with folate or 5dfol.

Finally, a complete structural explanation of product-off kinetics for ecDHFR must take the cofactor into account. As already mentioned, binding of a fresh molecule of NADPH to the ecDHFR·THF complex increases the THF-off rate by a factor of about 9. Earlier, we described the superimposition of the NADPH holoenzyme structure with each of the four binary complexes. We found that the enzyme is evidently designed to bind NADPH and THF so as to bring C4 of the nicotinamide and C7 of THF to within 1.8 Å of one another, a distance that represents a van der Waals overlap of approximately 2.0 Å. Such a large unfavorable interaction may well explain the acceleration of THF release by a bound NADPH.

ACKNOWLEDGMENT

We thank Dr. Huguette Pelletier for important suggestions regarding crystallographic refinement and Dr. Hyunsook Lee for valuable help in writing the Fortran 77 programs we used in analyzing our results.

REFERENCES

Anderson, D. H. (1987) Ph.D. Dissertation, Department of Physics, University of California, San Diego, La Jolla, CA 92037.

Blakley, R. L. (1984) in *Chemistry and Biochemistry of Folates, Vol. I: Folates and Pterins* (Blakley, R. L, & Benkovic, S. J., Eds.) pp 191−253, John Wiley & Sons, New York.

Blakley, R. L., & Appleman, J. R. (1994) *Adv. Enzymol.* (in press).

Blakley, R. L., Appleman, J. R., Freisheim, J. H., & Jablonsky, M. J. (1993) *Arch. Biochem. Biophys. 306*, 501−509.

Bolin, J. T., Filman, D. J., Matthews, D. A., Hamlin, R. C., & Kraut, J. (1982) *J. Biol. Chem. 257*, 13650−13662.

Brown, K. A., & Kraut, J. (1992) *Faraday Discuss. Chem. Soc. 93*, 217−224.

Bystroff, C., & Kraut, J. (1991) *Biochemistry 30*, 2227−2239.

Bystroff, C., Oatley, S. J., & Kraut, J. (1990) *Biochemistry 29*, 3263−3277.

Chen, Y. Q., Kraut, J., Blakley, R. L., & Callender, R. (1994) *Biochemistry 33*, 7021−7026.

Davies, J. F., II, Delcamp, T. J., Prendergast, N. J., Ashford, V. A., Freisheim, J. H., & Kraut, J. (1990) *Biochemistry 29*, 9467−9479.

Fierke, C. A., Johnson, K. A., & Benkovic, S. J. (1987) *Biochemistry 26*, 4085−4092.

Freisheim, J. H., & Matthews, D. A. (1984) in *Folate Antagonists as Therapeutic Agents* (Sirotnak, F. M., Burchall, J. J., Ensminger, W. D., & Montgomery, J. A., Eds.) Vol. 1, pp 69−131, Academic Press, Inc., Orlando, FL.

Gandour, R. D. (1981) *Bioinorg. Chem. 10*, 169−170.

Hamlin, R. (1985) *Methods Enzymol. 114*, 416−452.

Howell, E. E., Villafranca, J. E., Warren, M. S., Oatley, S. J., & Kraut, J. (1986) *Science 231*, 1123−1128.

Kraut, J. (1988) *Science 242*, 533−540.

Kraut, J., & Matthews, D. A. (1987) in *Biological Macromolecules and Assemblies* (Jurnak, F. A., & McPherson, A., Eds.) Vol. 3, pp 1−72, John Wiley & Sons, New York.

Kuyper, L. F. (1989) in *Computer-Aided Drug Design: Methods and Applications* (Perun, T. J., & Propst, C. L., Eds.) pp 327−369, Marcel Dekker, Inc., New York.

Li, L., Falzone, C. J., Wright, P. E., & Benkovic, S. J. (1992) *Biochemistry 31*, 7826−7833.

Luzzati, V. (1952) *Acta Crystallogr. 5*, 802−810.

Maharaj, G., Selinsky, B. S., Appleman, J. R., Perlman, M., London, R. E., & Blakley, R. L. (1990) *Biochemistry 29*, 4554−4560.

McTigue, M. A., Davies, J. F., II, Kaufman, B. T., & Kraut, J. (1992) *Biochemistry 31*, 7264−7273.

Morrison, J. F., & Stone, S. R. (1988) *Biochemistry 27*, 5499−5506.

Penner, M. H., & Frieden, C. (1987) *J. Biol. Chem. 262*, 15908−15914.

Rossmann, M. G., & Argos, P. (1975) *J. Biol. Chem. 250*, 7525−7532.

Sawaya, M. R. (1994) Ph.D. Dissertation, Department of Chemistry and Biochemistry, University of California, San Diego, La Jolla, CA 92037.

Smith, D. R., & Calvo, J. M. (1980) *Nucleic Acids Res. 8*, 2255−2274.

Smith, D. R., & Calvo, J. M. (1982) *Mol. Gen. Genet. 187*, 72−78.

Stone, S. R., & Morrison, J. F. (1988) *Biochemistry 27*, 5493−5499.

Tronrud, D. E., Ten Eyck, L. F., & Matthews, B. W. (1987) *Acta Crystallogr. A43*, 489−501.

Warren, M. S., Brown, K. A., Farnum, M. F., Howell, E. E., & Kraut, J. (1991) *Biochemistry 30*, 11092−11103.

Weast, R. C., Ed. (1968) *CRC Handbook of Chemistry and Physics*, 49th ed., p D-88, The Chemical Rubber Co., Cleveland, OH.

Williams, E. A., & Morrison, J. M. (1992) *Biochemistry 31*, 6801−6811.

Wu, Y. D., & Houk, K. N. (1987a) *J. Am. Chem. Soc. 109*, 906−908.

Wu, Y. D., & Houk, K. N. (1987b) *J. Am. Chem. Soc. 109*, 2226−2227.

Xuong, N. H., Nielsen, C. P., Hamlin, R., & Anderson, D. H. (1985) *J. Appl. Crystallogr. 18*, 342−350.

BI9422687